


2-anilino-4-amino-5-arylthiazole-type compound AS7128 inhibits lung cancer growth through decreased iASPP and p53 interaction

Hao-Wei Cheng¹ | Rong-Jie Chein² | Ting-Jen Cheng³ | Pei-Shan Wu⁴ |
Hsin-Yi Wu² | Pei-Fang Hung⁵ | Chia-Jen Wang⁶ | Yuan-Ling Hsu⁷ |
Jau-Min Wong^{1,8} | Ang Yuan^{8,9} | Chi-Huey Wong³ | Pan-Chyr Yang^{5,8} |
Szu-Hua Pan^{4,7,10} 

¹Institute of Biomedical Engineering, National Taiwan University, Taipei, Taiwan

²Institute of Chemistry, Academia Sinica, Taipei, Taiwan

³Genomics Research Center, Academia Sinica, Taipei, Taiwan

⁴Genome and Systems Biology Degree Program, National Taiwan University and Academia Sinica, Taipei, Taiwan

⁵Institute of Biomedical Sciences, Academia Sinica, Taipei, Taiwan

⁶Institute of Stem Cell and Translational Cancer Research, Chang Gung Memorial Hospital, Taoyuan, Taiwan

⁷Graduate Institute of Medical Genomics and Proteomics, National Taiwan University, Taipei, Taiwan

⁸Department of Internal Medicine, National Taiwan University Hospital, Taipei, Taiwan

⁹Department of Emergency Medicine, National Taiwan University Hospital, Taipei, Taiwan

¹⁰Doctoral Degree Program of Translational Medicine, National Taiwan University, Taipei, Taiwan

Correspondence

Szu-Hua Pan, Graduate Institute of Medical Genomics and Proteomics, National Taiwan University, Taipei, Taiwan.
Email: shpan@ntu.edu.tw

Funding information

National Taiwan University, Academia Sinica, Ministry of Science and Technology (Taiwan) (NSC 102-2314-B-002-046-MY3, 102-2923-B-002-004, 103-2923-B-002-003, MOST

Lung cancer is the leading cause of cancer-related death worldwide. Thus, developing novel therapeutic agents has become critical for lung cancer treatment. In this study, compound AS7128 was selected from a 2-million entry chemical library screening and identified as a candidate drug against non-small cell lung cancer in vitro and in vivo. Further investigation indicated that AS7128 could induce cell apoptosis and cell cycle arrest, especially in the mitosis stage. In addition, we also found that iASPP, an oncogenic protein that functionally inhibits p53, might be associated with AS7128 through mass identification. Further exploration indicated that AS7128 treatment could restore the transactivation ability of p53 and, thus, increase the expressions of its downstream target genes, which are related to cell cycle arrest and apoptosis. This occurs through disruption of the interactions between p53 and iASPP in cells. Taken together, AS7128 could bind to iASPP, disrupt the interaction between iASPP and p53, and result in cell cycle arrest and apoptosis. These findings may provide new insight for using iASPP as a therapeutic target for non-small cell lung cancer treatment.

KEYWORDS

apoptosis, cell cycle, iASPP, lung cancer, p53

This is an open access article under the terms of the Creative Commons Attribution-NonCommercial License, which permits use, distribution and reproduction in any medium, provided the original work is properly cited and is not used for commercial purposes.

© 2018 The Authors. *Cancer Science* published by John Wiley & Sons Australia, Ltd on behalf of Japanese Cancer Association.

105-2628-B-002-007-MY3, 106-0210-01-15-02, NTU-CDP-103R7879 and 104R7879); National Research Program for Biopharmaceuticals (ChemBank and High-Throughput Screening Resource Center, NSC 100-2325-B-001-022, NSC 101-2325-B-001-029 and NSC 102-2325-B-001-041).

1 | INTRODUCTION

Lung cancer remains the leading cause of cancer-related death worldwide.^{1,2} Although people are paying more attention to preventive medicine, an estimated 1.8 million new cases of lung cancer are diagnosed each year, and most of them are non-small cell lung cancer (NSCLC). Although target therapies are improving the clinical outcomes of lung cancer, the occurrence of drug resistance is a critical challenge.³ Thus, new therapeutics are needed.

In general, cancer occurs due to an alteration of cell division, which is an important process that lets cells grow, replicate their DNA and divide. The cell cycle process is usually controlled by complicated signaling pathways that include many regulators, such as p53. This regulator may protect the genome through its role in maintaining stability by ensuring that replication errors are corrected.⁴ As such, malfunctions of p53 may interfere with cell cycle arrest, apoptosis, senescence and autophagy.⁵

Several studies indicate that the activity of p53 is suppressed through binding of murine double minute 2 (MDM2) and inducing p53 proteasome degradation.⁶ In addition, a high mutation rate of p53 has been detected in a majority of cancers.⁷ The mutant p53 may acquire oncogenic functions through alterations in its DNA binding ability, changes in the associated protein network or interference with its downstream gene expressions.^{8,9} In addition to cell proliferation, p53 is involved in the regulation of the epithelial-to-mesenchymal transition and cancer stem cell features.¹⁰⁻¹² Hence, the restoration of wild-type p53 activity could be a path for developing novel anticancer therapeutics.

Emerging evidence shows that iASPP, which is encoded by the PPP1R13L gene, is overexpressed in various cancers.¹³⁻¹⁷ The family of apoptosis-stimulating proteins of p53 (ASPP) consists of ASPP1, ASPP2 and iASPP. The first 2 are considered as common activators of p53 that can enhance cell apoptosis, whereas iASPP acts as an inhibitor that can suppress the apoptotic transactivation potential of p53 by direct interaction.¹⁸ iASPP can also inhibit the apoptotic activity of p63 and p73 and promote p53-independent carcinogenesis.^{19,20}

In general, iASPP can be divided into 2 isoforms, which have 407 and 828 amino acids. The shorter one is a nuclear protein, and the longer one is located in both the cytosol and the nucleus.^{10,21} Nuclear iASPP may facilitate tumor progression and correlate with poor clinical outcome in prostate cancer and melanoma.^{22,23} All of the evidence suggests that targeting iASPP may be a feasible way to restore the function of p53. This idea was supported by 2 studies of

p53-derived peptides, 37AA and A34, which can disrupt the interaction of iASPP with p73 and p53, respectively.^{20,24}

Recently, a 2-step high-throughput screening of several lung cancer cells with different EGFR status was performed in our laboratory.^{25,26} AS7128, a 2-anilino-4-amino-5-arylthiazole compound, was one of the candidates selected for its activity against lung cancer cell growth with a reasonable therapeutic window compared with a control. In this study, we explored the potential mechanisms of AS7128 in vitro and in vivo. We present the interesting finding that AS7128 can inhibit lung cancer cell growth through restoring the activity of p53 by targeting iASPP. This may provide a new insight to develop novel therapeutics for NSCLC treatment in the future.

2 | MATERIALS AND METHODS

2.1 | Cell lines and culture conditions

The human lung cancer cell lines A549 (adenocarcinoma, ATCC CCL-185), H1975 (adenocarcinoma, ATCC CRL-5908), H460 (large cell carcinoma, ATCC HTB-177), H838 (adenocarcinoma, ATCC CRL-5844) and H1299 (adenocarcinoma, ATCC CRL-5803), and the foreskin fibroblast cell line Hs68 were purchased from the American Type Culture Collection (ATCC) (Manassas, VA, USA). A549 and Hs68 were grown in DMEM medium (Thermo Fisher Scientific, Rockford, IL, USA), and the other cell lines were grown in RPMI 1640 medium (Thermo Fisher Scientific) supplemented with 10% FBS (v/v), penicillin (100 units/mL) and streptomycin (100 µg/mL). The cells were grown at 37°C in a humidified atmosphere of 5% CO₂ and 95% air.

2.2 | Chemical library

The 2-million screening compound library contains commercial synthetic molecules, known bioactive inhibitors and approved drugs, pure natural products, and proprietary collections. The synthetic molecules in the 2-million library can be clustered into approximately 5300 groups, based on 85% structure similarity. The diversity is approximately 0.87, calculated using a modified centroid-diversity sorting algorithm. Compounds were prepared at 1 mmol/L in 100% DMSO in 1536-well propylene plates.

2.3 | Xenograft tumor growth in vivo

Experiments were carried out using BALB/c-nu mice, and all of the animal procedures were in accordance with the procedures and

guidelines of the Institutional Animal Care and Use Committee. A total of 3×10^6 H1975 human lung cancer cells were subcutaneously injected into the flank of 6-week-old BALB/c-nu mice (purchased from BioLABSCO, Yilan, Taiwan). Three days after the inoculation with cancer cells, the animals were divided into 4 groups. Seven days after tumor implantation, both vehicle and 3 doses of AS7128 were suspended in 50% PEG400 (in PBS) and given intraperitoneally to the animals twice a week for 18 days. Body weight and tumor size were measured each time before drug delivery.

The tumor volume was calculated using the largest diameters (a) and smallest diameters (b) as $V = 0.5 \times ab^2$. In addition, mice sera were collected to examine the levels of glutamate oxaloacetate transaminase (GOT), glutamate pyruvate transaminase (GPT), blood urine nitrogen (BUN) and creatinine (CREA) after the mice were sacrificed. HE stain was purchased from the National Taiwan University College of Medicine Laboratory Animal Center (Taipei, Taiwan). A POD In Situ Cell Death Detection Kit was used to determine the cell apoptosis in the tumor section according to the manufacturer's protocol (Roche Diagnostics, Indianapolis, IN, USA).

2.4 | Immunoprecipitation and protein identification

H1975 cells were lysed on ice in 20 mmol/L Tris (pH 8.0), 150 mmol/L NaCl, 100 μ mol/L Na_3VO_4 , 50 mmol/L NaF, 30 mmol/L sodium pyrophosphate and 0.5% NP-40. A 25-fold dilution of a stock solution was treated with a Mini Protease Inhibitor Cocktail Tablet (Roche Diagnostics) dissolved in 2 mL of distilled water, and clarified by centrifugation. The supernatants were taken as the total cell lysates. The compound-associated proteins were immunoprecipitated using AS7128 conjugated magnetic beads (which were synthesized as in Figure S1 and Data S1). The immunoprecipitated proteins were separated by SDS-PAGE, and the proteins were identified in a selected region by mass spectrometry.

The isolated gels were subjected to trypsin digestion and analyzed by mass spectrometry (LTQ-orbitrap XL; Institute of Biological Chemistry, Academia Sinica, Taiwan). The protein identification was processed by Proteome Discoverer software workflow (Thermo Fisher Scientific) using the Mascot search engine against the Swiss-Prot *Homo sapiens* protein database. Non-specific binding protein were eliminated from control group first. The remaining interactors were mapped using the CRAPome database²⁷ and a recent study²⁸ to determine the contaminant frequency of observations across AP-MS; and those frequency more than 15% were also be eliminated as the non-specific binders in this filter step. Then, the confidential interacting proteins were used to enrich their biological process annotations by Gene Ontology (GO) analysis; and we finally selected the potential targets more focusing on those related to apoptosis- and cell-cycle-related proteins (detailed proteins are listed in Tables S1 and S2).

2.5 | Real-time quantitative RT-PCR

Total RNA was extracted from cells and reverse transcribed using SuperScript III Reverse Transcriptase (Thermo Fisher Scientific) and

Random Hexamer primers (Thermo Fisher Scientific) in the presence of an RNase inhibitor according to the manufacturer's instructions. The detection primers of each gene are shown in Table S3. The reaction signals were detected by SYBR Green reagent (Thermo Fisher Scientific), and TATA-Box Binding Protein (TBP) was used as an internal control (GenBank X54993). The expression level of the detection gene relative to that of TBP was defined as $-\text{dCt} = -[\text{Ct of Gene} - \text{Ct of TBP}]$, and the ratio was calculated as $2^{-\text{dCt}}$. Experiments were performed in duplicate, and no-template controls were included in each assay.

2.6 | Statistical analysis

The data are presented as the means \pm SD or SEM, and the significance of differences was analyzed using Student's t test. All experiments were performed in triplicate, the statistical testing was 2-tailed, and $P < .05$ was considered statistically significant.

The details of other methods are listed in Data S1.

3 | RESULTS

3.1 | Identification of AS7128 that possesses non-small cell lung cancer inhibitory activities

Through high-throughput screening, we identified the 2-anilino-4-amino-5-arylthiazole-type compound AS7128, which has the chemical structure shown in Figure 1A. AS7128 could inhibit the viabilities of several lung cancer cells with IC_{50} values of 0.1–0.3 μ mol/L. Furthermore, it has 10 times higher potency for cancer cells than normal cells (Figure 1B). This suggests that AS7128 has potential for lung cancer treatment. As such, we further investigated its anti-tumor efficacy in vivo.

Athymic nude mice bearing established subcutaneous H1975 tumors were intraperitoneally treated with DMSO (as a control) or 0.5, 1 and 3 mg/kg of AS7128 twice a week for 18 days. The body weight and tumor volume were monitored for each treatment time period. The results showed that treatment with AS7128 significantly inhibited H1975 xenograft tumor growth compared with the control without altering the body weight between the 4 groups ($n = 4$ for each group; average tumor size, $1625.4 \pm 493.5 \text{ mm}^3$ for DMSO, $1029.3 \pm 202.4 \text{ mm}^3$ for 0.5 mg/kg, $700.4 \pm 136.6 \text{ mm}^3$ for 1 mg/kg and $611.7 \pm 288.9 \text{ mm}^3$ for 3 mg/kg on day 24; $P = .014$ for 1 mg/kg and 0.018 for 3 mg/kg, both compared with the DMSO control; Figure 1C,D).

HE staining and TUNEL assay analysis revealed that AS7128 inhibits tumor growth and induces apoptosis in the tumor region (Figure 1E,F). In addition, mice sera were collected to perform biochemical analyses of GOT, GPT, BUN and CREA to evaluate cytotoxicity of AS7128 (with focus on the effects on the liver and kidney). The results showed that there was no statistical difference between the control and the 3 treated groups (Figure S2). These results suggest that AS7128 could inhibit tumor growth in vitro and in vivo.

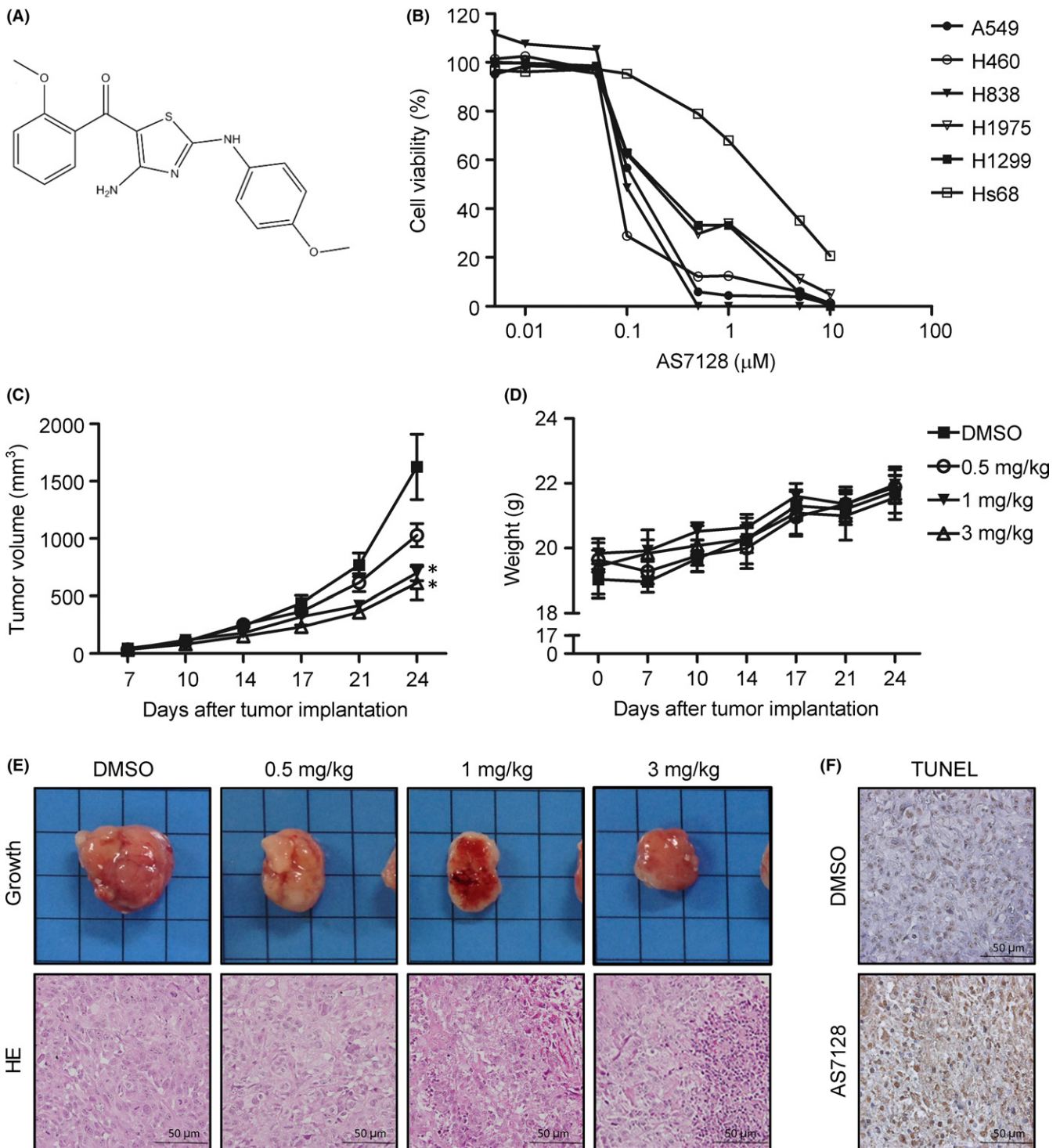


FIGURE 1 Tumor growth inhibition by AS7128 in vitro and in vivo. A, Chemical structure of AS7128. B, The cell viability of different lung cancer cell lines against AS7128 was determined by SRB assay after 72 h of treatment. Hs68: normal fibroblast. Experiments were performed in triplicate. C, D, Nude mice were subcutaneously injected with 3×10^6 H1975 cells. Mice were treated with DMSO, 0.5, 1 or 3 mg/kg of AS7128 intraperitoneally twice a week for 18 d after 7 d of tumor implantation. Mice tumor volume (C) and body weight (D) were monitored twice a week. The data are presented as the mean \pm SEM and were analyzed using Student's *t*-test. Asterisks represent statistically significant differences ($*P < .05$). E, Tumor photographs after sacrifice (upper panel). Scale: 1 cm. Tissue morphology was examined by HE staining (lower panels). Scale: 50 μ m. F, Cell apoptosis status was examined by TUNEL staining. Scale: 50 μ m

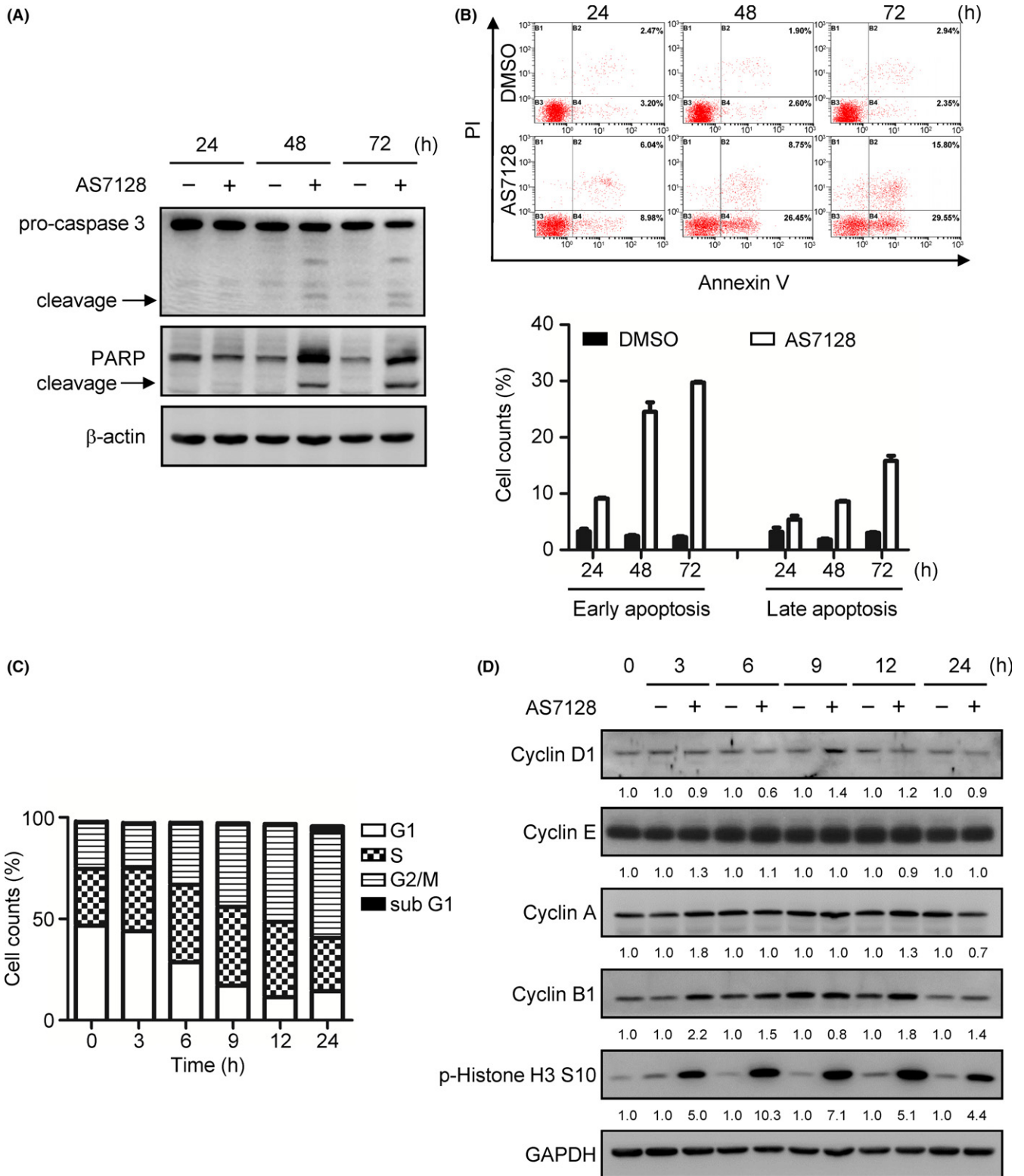


FIGURE 2 Induction of apoptosis and cell cycle arrest by AS7128 in H1975 cells. H1975 cells were treated with 250 nmol/L of AS7128 for the indicated time. Apoptosis and cell cycle status were determined by the following experiments. A, Cleaved Caspase 3 and PARP were detected by immunoblotting. β -actin was used as the loading control. B, Cells were harvested for annexin V-PI double staining and evaluated for cell apoptosis by flow cytometry. The bar graphs reveal the apoptotic percentage of H1975 cells with AS7128 treatment. C, AS7128-treated cells were stained with PI to analyze the DNA content by flow cytometry. D, Expressions of indicated proteins of H1975 cells were detected by immunoblotting. GAPDH was used as the loading control. The densitometry value was measured by ImageJ. The data are presented as the mean \pm SD. Experiments were performed in triplicate

3.2 | AS7128 induced cell apoptosis and cell cycle arrest in H1975 cells

To understand the action mechanism of AS7128, we investigated whether the cytotoxic effect was due to cell apoptosis. The immunoblotting showed that cleavage caspase-3 and PARP, 2 important apoptotic markers, appeared after H1975 cells were treated with AS7128 (Figure 2A). In addition, the flow cytometry examination indicated that the positive staining population of both annexin V and PI increased in AS7128-treated H1975 cells (29.55% of treated cells vs 2.35% of the control group and 15.80% of treated cells vs 2.94% of the control group in early and late apoptosis, respectively, at 72 hour; Figure 2B). The data suggest that AS7128 treatment causes apoptosis in lung cancer cells.

We next explored whether the apoptotic effect of AS7128 treatment was derived from unregulated cell proliferation. The results indicated that the cell population of AS7128-treated H1975 cells was significantly decreased in the G1 stage and increased in the G2/M stages in asynchronous conditions (Figure 2C). The compound would, thus, induce a sub-G1 population of H1975 cells.

We also examined the expression levels of several cell cycle checkpoints, including cyclin D1, E, A and B1 and phospho-histone H3. As shown in Figure 2D, the expressions of cyclin B1 and serine 10 in phospho-histone H3 were increased after H1975 cells were treated with AS7128. Collectively, the data suggest that treatment with AS7128 might induce cell apoptosis through cell cycle G2/M arrest in H1975 cells.

3.3 | AS7128 arrested H1975 cell in M phase

To examine the events of AS7128-induced cell cycle arrest, H1975 cells were synchronized at the G1/S transition by double thymidine block and subsequently released into fresh medium containing DMSO or 250 nmol/L of AS7128 for 12 hour. The cell cycle statuses were monitored each hour by measuring the DNA contents with PI staining. As expected, cells treated with AS7128 were arrested in the G2/M phases, but most of the control cells re-entered the G1 phase at 12 hour after release (Figure 3A).

We reperformed the same experiment and extended the releasing time to 18 hour to clarify whether the arrested H1975 cells could pass the G2/M phases after releasing for 12 hour under AS7128 treatment. The results showed that most of the H1975 cells were still arrested in the G2/M phases after 18 hour of release with AS7128 treatment (Figure S3). This result was further confirmed by examining the protein expression levels of different cell cycle checkpoints. As

shown in Figure 3B, the expressions of cyclin B1 and serine 10 in phospho-histone H3 (2 specific G2 and M phase markers) were significantly increased in treated cell lysates compared with the control.

Next, we examined how AS7128 treatment induced G2/M arrest in cells. The cyclin B-cdc2 complex is required for the G2/M transition. Activation of the cyclin B-cdc2 complex may trigger cells to enter the M phase. This activation comprises several steps, including cdc2 dephosphorylation at Thr14 and Tyr15 and phosphorylation at Thr161.²⁹ To investigate whether the AS7128 treatment could interfere with the steps of G2/M transition, H1975 cells were synchronized at the G1/S stage by double thymidine block and released into fresh medium with or without AS7128. Protein extracts were collected to analyze the phosphorylation levels of cdc2 at Tyr15 and Thr161at each indicated time point.

Surprisingly, both the AS7128-treated and DMSO control groups presented similar patterns of these 2 phosphorylation statuses (Figure 3C). This implied that AS7128 treatment may cause incomplete M phase progression in H1975 cells. To test our hypothesis, we focused on the effect of AS7128 treatment during the mitosis processes. Similarly, H1975 cells were synchronized and released with or without AS7128 treatment. Cells were fixed and stained with DAPI and then cells with different chromosome arrangements were counted in at least 12 fields to analyze the percentage of each mitotic stage, including interphase, prophase, and after prometaphase.

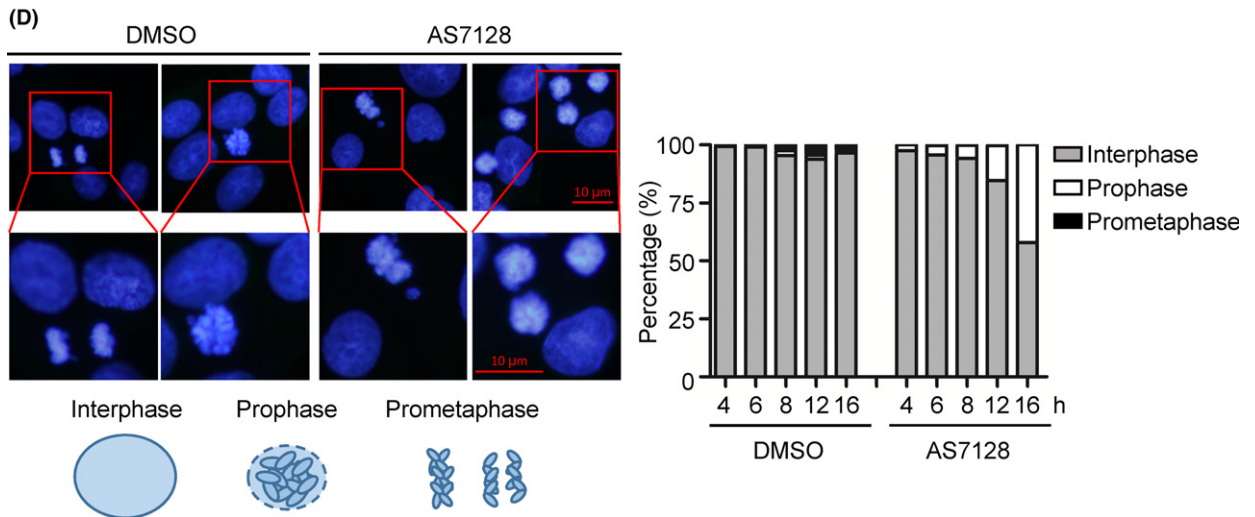
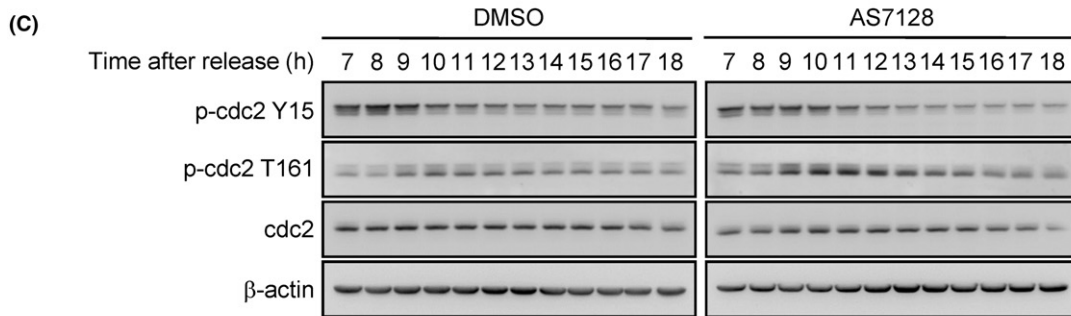
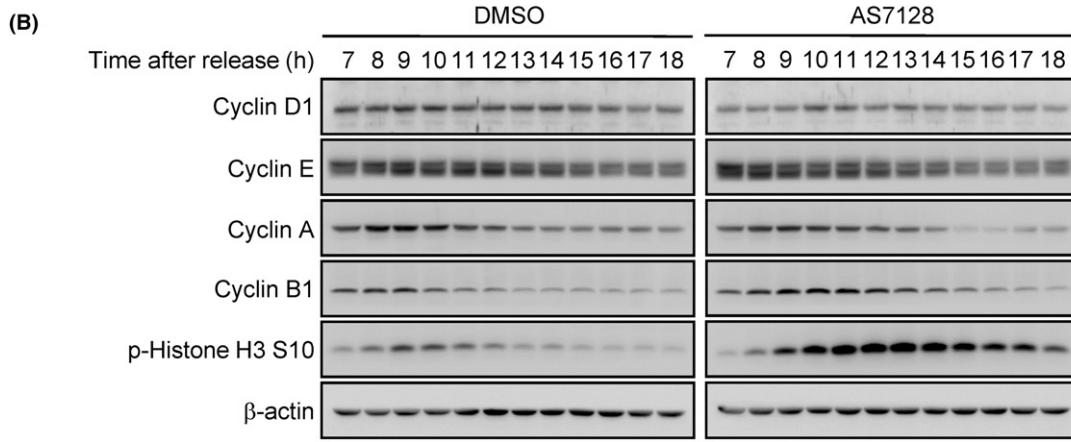
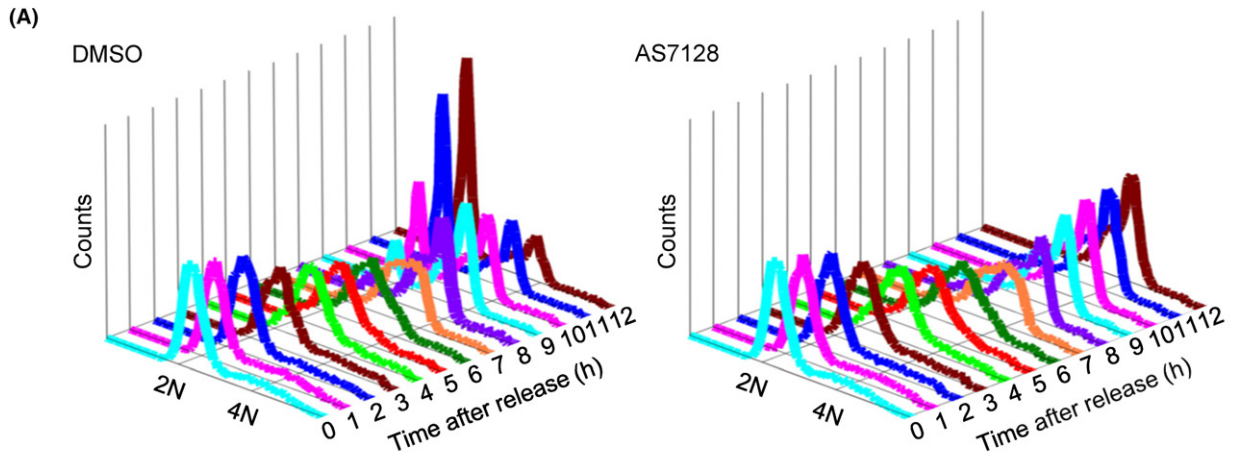
The criteria for the 3 phases are shown below the fluorescence image, and the results are presented as histograms (Figure 3D). Compared with the DMSO group, the percentage of prophase cells was significantly higher in the AS7128-treated group in a time-dependent manner. Taken together, the data suggest that treatment with AS7128 may lead to the arrest of H1975 cells in the prophase mitotic stage.

3.4 | iASPP might be the action target of AS7128

Because AS7128 treatment could cause cell cycle arrest in the prophase and induce cell apoptosis, we investigated its mechanism of action. AS7128 was conjugated into magnetic beads (Figure 4A) and used to identify potential targets in H1975 lung cancer cells. The pull-down samples were separated by 2 SDS-PAGEs with different concentrations of acrylamide. Seven regions with significantly different protein expressions were selected for protein identification by LC/MS-MS (Figure S4A).

A total of 527 proteins were identified, of which 390 showed significantly differential expressions in the AS7128-treated group after filtering out non-specific binding proteins with over 15%

FIGURE 3 M phase arrest in H1975 cells by AS7128. H1975 cells were synchronized in the G1/S stage by double thymidine and released with medium containing DMSO or 250 nmol/L AS7128. Cells were harvested, and the cell cycle status was estimated at indicated times by the following experiments. A, Stages of the cell cycle were determined by flow cytometry to analyze the DNA content by PI staining. B, C, Expressions of cell-cycle-related proteins of H1975 cells were determined by immunoblotting. β -actin was used as the loading control. D, H1975 cells were fixed and stained with DAPI. The images were examined by fluorescence microscope. The bar graphs reveal the percentage of H1975 cells with different mitotic phases, as indicated by the criteria below the pictures. Scale: 10 μ m



frequency according to Marcon and Mellacheruvu's research.^{27,28} In addition, GO enrichment analysis revealed that 36 of these proteins were involved in cell apoptosis or cell cycle regulation (Figure S4B and Table S2). Among them, we chose the 2 proteins iASPP and CSE1L for further validation, which are related to p53-induced cell apoptosis. The results showed that iASPP but not CSE1L could be co-immunoprecipitated with AS7128 conjugated magnetic beads (Figure 4B and Figure S4C; NIH-3T3 was loaded as an antibody positive control). This implied that iASPP might be a potential target for AS7128 treatment in lung cancer.

3.5 | AS7128 could restore p53 function through disruption of the interaction between p53 and iASPP

A previous study indicated that the expression of iASPP could inhibit cell apoptosis through the binding of p53.³⁰ We wondered whether AS7128-induced cell apoptosis would result in interruption of the interaction between iASPP and p53. To test this hypothesis, the interaction between iASPP and p53 was detected by co-immunoprecipitation assays with or without AS7128 treated with H460 cells. The results showed that the binding of iASPP and p53 was inhibited under AS7128 treatment (Figure 4C) and also in p53 mutated H1975 cells (Figure S5).

We also examined whether the transactivation activity of p53 could be restored when AS7128 disrupted the iASPP-p53 interaction. As expected, the transactivation activity of p53 could be restored and presented nearly a 1.6-fold increase in the reporter assay (Figure 4D). In addition, the mRNA and protein expression levels of p53 downstream genes were significantly upregulated after treatment with AS7128 for 24 and 48 hour (Figures 4E,F and Figure S6). This treatment also induced cell apoptosis via PARP cleavage (Figure 4G) in both A549 and H460 cells. The data suggest that AS7128 could bind to iASPP, disrupt the interaction between iASPP and p53, and result in cell cycle arrest and apoptosis through restoring the transactivation activity of p53 and turning on the expressions of its downstream target genes in lung cancer cells (Figure 5).

4 | DISCUSSION

Despite treatment advances made over the past 20 years, the prognosis of lung cancer remains poor.^{31,32} Thus, new anticancer drugs are being developed to target certain molecular pathways, such as epidermal growth factor receptor (EGFR) or p53 signaling. We

identified a small molecule, AS7128, that could inhibit lung cancer cell growth in vitro and in vivo. Treatment with AS7128 led to cell cycle arrest in the mitosis stage and induced cell apoptosis. AS7128 could also be associated with the oncogenic protein iASPP and restore the transactivation ability of p53. This increases the expressions of downstream target genes, which are related to cell cycle arrest and apoptosis, through disruption of the interaction between p53 and iASPP in cells. AS7128 may, therefore, serve as a novel strategy for lung cancer treatment.

AS7128 is a type of 2-acrylamino-4-amino-5-arylothiazole compound, and has been reported as a new class of inhibitors of tubulin polymerization.³³ Romagnoli et al. report that the inhibition of tubulin polymerization of 2-anilino-4-amino-5-arylothiazoles might occur through binding to the colchicine site. For this reason, we tested whether AS7128 treatment could interfere with the dynamics of microtubules in our studies. As expected, AS7128 could cause tubulin depolymerization and delay microtubule regrowth after cold treatment in lung cancer cells (Figure S7). However, it is very interesting that our protein identification indicated that candidates other than tubulin could be potential targets for AS7128. Using AS7128-conjugated beads and mass spectrometry identification, we found that iASPP was presented in the pull-down complex of AS7128. Previous studies showed that iASPP is overexpressed in NSCLC, gastric cancer and cervical cancer, and it is correlated with pathological stages. Downregulation of iASPP could inhibit cell proliferation, invasion and migration, and it induced cell apoptosis.^{14,34-36} Moreover, iASPP could suppress both p53-dependent and independent apoptotic activity through interaction with p53, p63 or p73.¹⁸⁻²⁰ Thus, iASPP could be a suitable drug target for lung cancer therapy.

p53 is critical for regulating the cell cycle and apoptosis, and it is also known as a classical tumor suppressor, with over 50% human cancers carrying loss-of-function mutations.³⁷ As such, reactivation of p53 is one direction for the development of new therapeutic strategies for cancer treatment. Some approaches have been used to reactivate wild-type (Wt) or mutant (Mt) p53. Virus-based Wt p53 gene therapy provides functional p53 and induces cell apoptosis to enhance anticancer activity.^{38,39} Moreover, some small molecules have been reported to restore the function of Wt p53 by blocking the interaction between MDM2/MDM4 and p53, inhibiting the E3 ligase activity of MDM2, blocking SIRT to increase the stability of p53, or inhibiting the nuclear export of p53.^{40,41} Some of these molecules are being clinically evaluated.

We demonstrated that AS7128 could restore the transactivity of p53 through disrupting the interaction between p53 and its inhibitor,

FIGURE 4 Activated p53 and downstream genes through reduced interaction between iASPP and p53 under AS7128 treatment. A, Structure of compound conjugated magnetic beads. B, Association between AS7128 and iASPP was validated by immunoprecipitation and immunoblotting in H1975 cells. C, Reduced interaction between iASPP and p53 under AS7128 treatment was verified by endogenous immunoprecipitation and immunoblotting in H460 cells. D, Increased transactivation activity of p53 under AS7128 treatment was examined by luciferase reporter assay in H460 cells. E, F, Increased mRNA (after 48 h treatment) (E) and protein (F) expression of p53 downstream genes under AS7128 treatment were determined by RT-qPCR and immunoblotting, respectively. β -actin was used as the loading control. The densitometry value was measured by ImageJ. G, Cleaved PARP was detected by immunoblotting after AS7128 treatment. β -actin was used as the loading control. The data are presented as the mean \pm SD. Experiments were performed in triplicate (* $P < .05$)

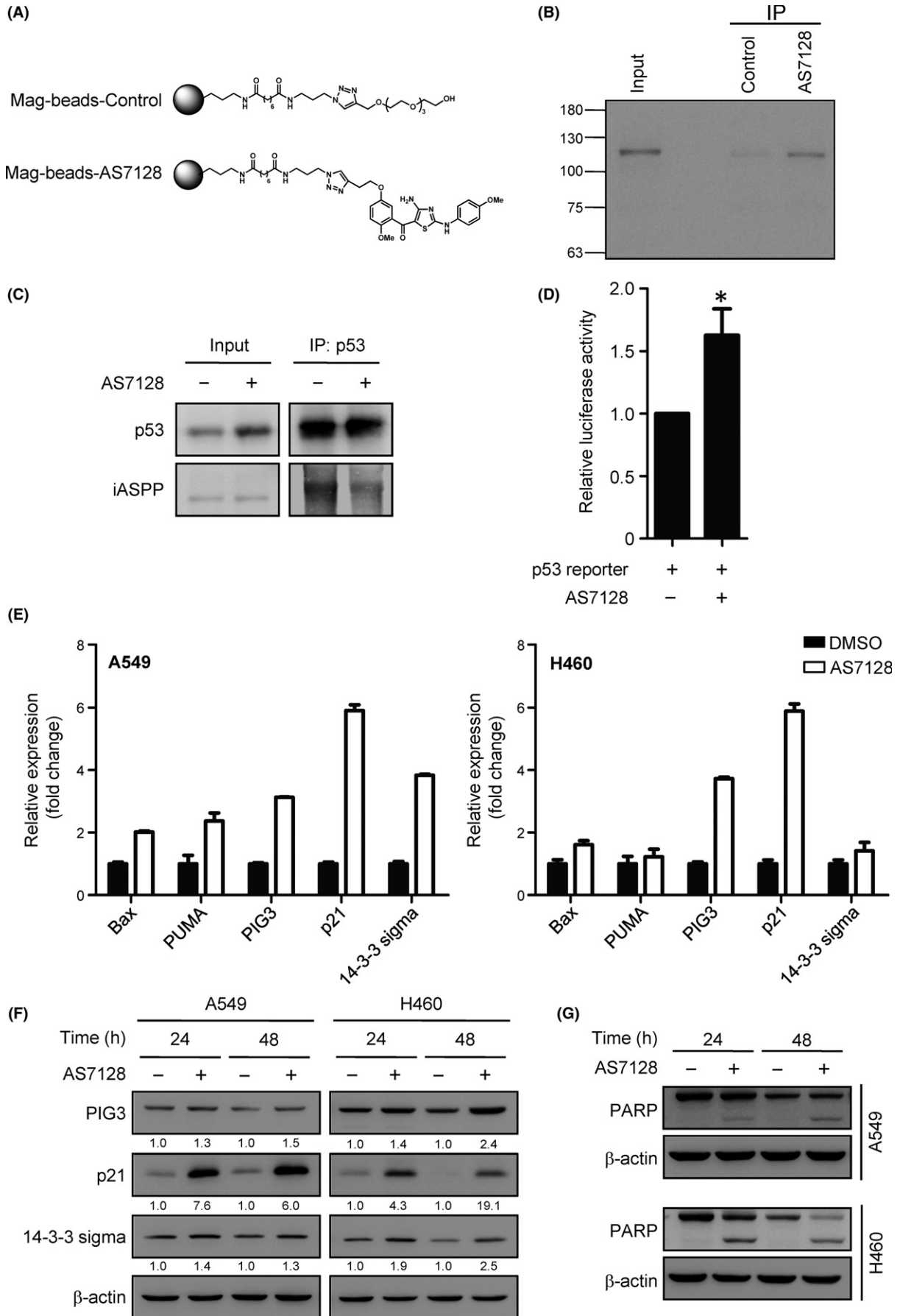
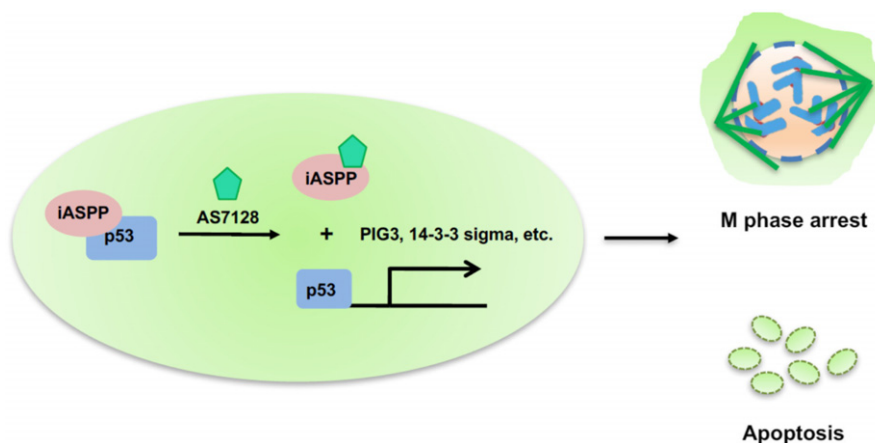


FIGURE 5 Schematic mechanism of AS7128 in lung cancer treatment. AS7128 enhanced the transactivation ability of p53 through decreasing the interaction between iASPP and p53, drove the gene expression of p53 downstream genes, and induced cell cycle M phase arrest and apoptosis



iASPP. In comparison with virus-based p53 injection, using small compounds would be more convenient and economical. Although the activation of p53 is required in anticancer treatment, p53-mediated apoptosis may be harmful in normal tissues. For example, hypoxia could induce ischemia.⁴² Furthermore, most p53 inhibitors like MDM2 or iASPP are usually overexpressed and act as an oncogene in cancers.^{14,37,43} Therefore, regulating p53 activity by targeting its inhibitors may be safer than using p53 itself. Thus, developing novel drugs that target iASPP might be a good option for restoring the function of p53 in cancer treatment.

The small peptides 37AA and A34 derived from p53 can increase the expression of p53 downstream genes, dissociate p73 or p53 from iASPP, and suppress tumor growth in vitro and in vivo.^{20,24} Silencing the expressions of iASPP could not only inhibit cell proliferation in vitro and tumor growth in vivo, but also upregulate the mRNA expression levels of p21 and PUMA.^{14,34} When we used siRNA to mimic the effect of AS7128 on targeting iASPP, we found that the mRNA and protein levels of BAX and 14-3-3 sigma were also upregulated in iASPP-silenced A549 and H460 cells (Figure S8). This suggests that iASPP is, indeed, a potential target for inhibiting lung cancer cell growth. Furthermore, miR-124 and miR-140 could regulate the expression levels of iASPP, as well as inhibit tumor growth in cervical cancer and glioma, respectively.^{35,44} We showed that treatment with AS7128 inhibited tumor growth in vitro and in vivo, as well as upregulated the expression levels of p53 downstream genes by disrupting the interaction between p53 and iASPP. Using a small molecule is a better way to reduce the costs of synthesis and storage and increase the delivery efficiency in clinical applications.

In conclusion, we identified the compound AS7128, which could bind to the oncoprotein iASPP, disrupt the interaction between iASPP and p53, and restore the function of p53 by activating the expression of p53 downstream genes and inducing cell apoptosis. Because p53 is an important tumor suppressor gene, reactivation of p53 function is proposed as an ideal approach for lung cancer therapy. The identification of AS7128 as an anti-lung cancer small molecule through reactivating p53 by targeting iASPP may provide new insight for further development of lung cancer treatments.

ACKNOWLEDGMENTS

The authors thank the following individuals for providing technical support: Dr Yih-Leong Chang and Dr Chen-Tu Wu (Department of Pathology and Graduate Institute of Pathology, College of Medicine, National Taiwan University).

CONFLICT OF INTEREST

The authors have no conflicts of interest to declare.

ORCID

Szu-Hua Pan  <http://orcid.org/0000-0002-0138-0434>

REFERENCES

1. Siegel RL, Miller KD, Jemal A. Cancer statistics, 2017. *CA Cancer J Clin.* 2017;67:7-30.
2. Torre LA, Bray F, Siegel RL, Ferlay J, Lortet-Tieulent J, Jemal A. Global cancer statistics, 2012. *CA Cancer J Clin.* 2015;65:87-108.
3. Jia Y, Yun CH, Park E, et al. Overcoming EGFR(T790M) and EGFR (C797S) resistance with mutant-selective allosteric inhibitors. *Nature.* 2016;534:129-132.
4. Read AP, Strachan T. *Human Molecular Genetics 2.* New York, NY: Wiley; 1999.
5. Zilfou JT, Lowe SW. Tumor suppressive functions of p53. *Cold Spring Harb Perspect Biol.* 2009;1:a001883.
6. Shi D, Gu W. Dual roles of MDM2 in the regulation of p53: ubiquitination dependent and ubiquitination independent mechanisms of MDM2 repression of p53 activity. *Genes Cancer.* 2012;3:240-248.
7. Olivier M, Hollstein M, Hainaut P. TP53 mutations in human cancers: origins, consequences, and clinical use. *Cold Spring Harb Perspect Biol.* 2010;2:a001008.
8. Kato S, Han SY, Liu W, et al. Understanding the function-structure and function-mutation relationships of p53 tumor suppressor protein by high-resolution missense mutation analysis. *Proc Natl Acad Sci USA.* 2003;100:8424-8429.
9. Muller PA, Vousden KH. p53 mutations in cancer. *Nat Cell Biol.* 2013;15:2-8.

10. Dong P, Ihira K, Hamada J, et al. Reactivating p53 functions by suppressing its novel inhibitor iASPP: a potential therapeutic opportunity in p53 wild-type tumors. *Oncotarget*. 2015;6:19968-19975.
11. Bieging KT, Mello SS, Attardi LD. Unravelling mechanisms of p53-mediated tumour suppression. *Nat Rev Cancer*. 2014;14:359-370.
12. Godar S, Ince TA, Bell GW, et al. Growth-inhibitory and tumor-suppressive functions of p53 depend on its repression of CD44 expression. *Cell*. 2008;134:62-73.
13. Saebo M, Skjelbred CF, Nexø BA, et al. Increased mRNA expression levels of ERCC1, OGG1 and RAI in colorectal adenomas and carcinomas. *BMC Cancer*. 2006;6:208.
14. Chen J, Xie F, Zhang L, Jiang WG. iASPP is over-expressed in human non-small cell lung cancer and regulates the proliferation of lung cancer cells through a p53 associated pathway. *BMC Cancer*. 2010;10:694.
15. Li G, Wang R, Gao J, Deng K, Wei J, Wei Y. RNA interference-mediated silencing of iASPP induces cell proliferation inhibition and G0/G1 cell cycle arrest in U251 human glioblastoma cells. *Mol Cell Biochem*. 2011;350:193-200.
16. Liu Z, Zhang X, Huang D, et al. Elevated expression of iASPP in head and neck squamous cell carcinoma and its clinical significance. *Med Oncol*. 2012;29:3381-3388.
17. Lu B, Guo H, Zhao J, et al. Increased expression of iASPP, regulated by hepatitis B virus X protein-mediated NF-kappaB activation, in hepatocellular carcinoma. *Gastroenterology*. 2010;139:2183-2194 e5.
18. Sullivan A, Lu X. ASPP: a new family of oncogenes and tumour suppressor genes. *Br J Cancer*. 2007;96:196-200.
19. Cai Y, Qiu S, Gao X, Gu SZ, Liu ZJ. iASPP inhibits p53-independent apoptosis by inhibiting transcriptional activity of p63/p73 on promoters of proapoptotic genes. *Apoptosis*. 2012;17:777-783.
20. Bell HS, Dufes C, O'Prey J, et al. A p53-derived apoptotic peptide derepresses p73 to cause tumor regression *in vivo*. *J Clin Invest*. 2007;117:1008-1018.
21. Bell HS, Ryan KM. iASPP inhibition: increased options in targeting the p53 family for cancer therapy. *Cancer Res*. 2008;68:4959-4962.
22. Morris EV, Cerundolo L, Lu M, et al. Nuclear iASPP may facilitate prostate cancer progression. *Cell Death Dis*. 2014;5:e1492.
23. Lu M, Breysens H, Salter V, et al. Restoring p53 function in human melanoma cells by inhibiting MDM2 and cyclin B1/CDK1-phosphorylated nuclear iASPP. *Cancer Cell*. 2013;23:618-633.
24. Qiu S, Cai Y, Gao X, Gu SZ, Liu ZJ. A small peptide derived from p53 linker region can resume the apoptotic activity of p53 by sequestering iASPP with p53. *Cancer Lett*. 2015;356(2 Pt B):910-917.
25. Kuo TC, Li LW, Pan SH, et al. Purine-type compounds induce microtubule fragmentation and lung cancer cell death through interaction with katanin. *J Med Chem*. 2016;59:8521-8534.
26. Yeh CT, Wu AT, Chang PM, et al. Trifluoperazine, an antipsychotic agent, inhibits cancer stem cell growth and overcomes drug resistance of lung cancer. *Am J Respir Crit Care Med*. 2012;186:1180-1188.
27. Mellacheruvu D, Wright Z, Couzens AL, et al. The CRAPome: a contaminant repository for affinity purification-mass spectrometry data. *Nat Methods*. 2013;10:730-736.
28. Marcon E, Jain H, Bhattacharya A, et al. Assessment of a method to characterize antibody selectivity and specificity for use in immunoprecipitation. *Nat Methods*. 2015;12:725-731.
29. Dunphy WG. The decision to enter mitosis. *Trends Cell Biol*. 1994;4:202-207.
30. Bergamaschi D, Samuels Y, O'Neil NJ, et al. iASPP oncoprotein is a key inhibitor of p53 conserved from worm to human. *Nat Genet*. 2003;33:162-167.
31. Nguyen KS, Kobayashi S, Costa DB. Acquired resistance to epidermal growth factor receptor tyrosine kinase inhibitors in non-small-cell lung cancers dependent on the epidermal growth factor receptor pathway. *Clin Lung Cancer*. 2009;10:281-289.
32. Nguyen KS, Neal JW. First-line treatment of EGFR-mutant non-small-cell lung cancer: the role of erlotinib and other tyrosine kinase inhibitors. *Biologics*. 2012;6:337-345.
33. Romagnoli R, Baraldi PG, Carrion MD, et al. 2-Arylamino-4-amino-5-aryloxythiazoles. "One-pot" synthesis and biological evaluation of a new class of inhibitors of tubulin polymerization. *J Med Chem*. 2009;52:5551-5555.
34. Wang LL, Xu Z, Peng Y, Li LC, Wu XL. Downregulation of inhibitor of apoptosisstimulating protein of p53 inhibits proliferation and promotes apoptosis of gastric cancer cells. *Mol Med Rep*. 2015;12:1653-1658.
35. Dong P, Xiong Y, Watari H, et al. Suppression of iASPP-dependent aggressiveness in cervical cancer through reversal of methylation silencing of microRNA-124. *Sci Rep*. 2016;6:35480.
36. Kong F, Shi X, Li H, et al. Increased expression of iASPP correlates with poor prognosis in FIGO IA2-IIA cervical adenocarcinoma following a curative resection. *Am J Cancer Res*. 2015;5:1217-1224.
37. Ozaki T, Nakagawara A. Role of p53 in cell death and human cancers. *Cancers (Basel)*. 2011;3:994-1013.
38. Liu TJ, el-Naggar AK, McDonnell TJ, et al. Apoptosis induction mediated by wild-type p53 adenoviral gene transfer in squamous cell carcinoma of the head and neck. *Cancer Res*. 1995;55:3117-3122.
39. Clayman GL, el-Naggar AK, Roth JA, et al. *In vivo* molecular therapy with p53 adenovirus for microscopic residual head and neck squamous carcinoma. *Cancer Res*. 1995;55:1-6.
40. Selivanova G. Wild type p53 reactivation: from lab bench to clinic. *FEBS Lett*. 2014;588:2628-2638.
41. Bykov VJN, Wiman KG. Mutant p53 reactivation by small molecules makes its way to the clinic. *FEBS Lett*. 2014;588:2622-2627.
42. Vousden KH, Prives C. Blinded by the light: the growing complexity of p53. *Cell*. 2009;137:413-431.
43. Wade M, Li YC, Wahl GM. MDM2, MDMX and p53 in oncogenesis and cancer therapy. *Nat Rev Cancer*. 2013;13:83-96.
44. Zhao H, Peng R, Liu Q, et al. The lncRNA H19 interacts with miR-140 to modulate glioma growth by targeting iASPP. *Arch Biochem Biophys*. 2016;610:1-7.

SUPPORTING INFORMATION

Additional Supporting Information may be found online in the supporting information tab for this article.

How to cite this article: Cheng H-W, Chein R-J, Cheng T-J, et al. 2-anilino-4-amino-5-aryloxythiazole-type compound AS7128 inhibits lung cancer growth through decreased iASPP and p53 interaction. *Cancer Sci*. 2018;109:832-842. <https://doi.org/10.1111/cas.13489>